

Cite this: *Chem. Commun.*, 2011, **47**, 2032–2034

www.rsc.org/chemcomm

## Nb doping of TiO<sub>2</sub> nanotubes for an enhanced efficiency of dye-sensitized solar cells†

Min Yang,<sup>a</sup> Doohun Kim,<sup>a</sup> Himendra Jha,<sup>a</sup> Kiyong Lee,<sup>a</sup> Jonathan Paul<sup>b</sup> and Patrik Schmuki\*<sup>a</sup>

Received 16th November 2010, Accepted 6th December 2010

DOI: 10.1039/c0cc04993j

**Nb-doped TiO<sub>2</sub> nanotube (with C<sub>Nb</sub> < 1 wt%) layers were successfully fabricated by self-ordered electrochemical anodization of Ti–Nb alloys. When used in dye-sensitized solar cells the efficiency enhanced by up to 30% compared to non-doped TiO<sub>2</sub> nanotubes. IMVS measurements indicate the beneficial effect to be due to lower recombination losses.**

Since dye-sensitized solar cells (DSSC) based on photosensitization of TiO<sub>2</sub> nanoparticles were first designed by Grätzel and O'Regan in 1991,<sup>1</sup> the concept has become one of the most promising alternative candidates to Si-based photovoltaic cells. In DSSCs, visible solar light is captured by a HOMO–LUMO transition in a suitable dye, adsorbed on a TiO<sub>2</sub> nanostructure. After electron transfer to the TiO<sub>2</sub> conduction band, the TiO<sub>2</sub> serves as an electron conductor to a back-contact. In the classical Grätzel cell a compact layer of TiO<sub>2</sub> nanoparticles is used as an electron carrier. Factors that limit the conversion efficiency in such DSSCs are the comparably slow electron transport and a considerably high defect density in the TiO<sub>2</sub> nanostructure (facilitating carrier recombination losses).<sup>2,3</sup> Over the past decade, many attempts were made to replace the nanoparticle system by one-dimensional TiO<sub>2</sub> nanostructures such as nanowires,<sup>4,5</sup> nanofibers,<sup>6</sup> or nanorods,<sup>7</sup> in order to improve the electron transport efficiency. In the past few years, particularly self-organized nanotube layers were increasingly investigated. In this context, self-ordered TiO<sub>2</sub> nanotubes (NT) have shown some excellent properties.<sup>8–11</sup> In order to further improve the electronic properties of TiO<sub>2</sub>, a very interesting path seems to be efforts to dope the material with beneficial secondary species. A particularly interesting doping species in TiO<sub>2</sub> is Nb-oxide that has been shown to increase photoemission properties,<sup>12</sup> or enhance the life time of polymer solar cells.<sup>13</sup> However, most striking are recent reports on a significant modification of the conductivity in TiO<sub>2</sub> by minor Nb<sub>2</sub>O<sub>5</sub>

additions.<sup>14,15</sup> Effects of low concentration doping with Nb are mostly ascribed to Nb<sup>5+</sup> that lead to mixed Nb4d–Ti3d states close to the TiO<sub>2</sub> conduction band<sup>12</sup>—these states are considered for concentration < 6% as 90% efficient ionized donors. For smaller amount of Nb (~0.2%) an increasing Hall mobility with temperature has been reported which makes such a material combination highly interesting to be explored in electron conducting devices.<sup>12</sup>

In the present work we explore the feasibility to grow directly anodic Nb-doped TiO<sub>2</sub> nanotube (NT) layers using TiNb alloys with low Nb contents (0.02 to 1.0 wt%) and use them in DSSCs. We show not only that the self-ordered TiO<sub>2</sub> NT array doped with Nb contents can be grown but also that Nb doping can lead to a significantly enhanced performance of the solar cell.

To grow Nb doped nanotube layers we used Nb–Ti alloys (0.02 to 1.0 wt%) and anodized them in an ethylene glycol electrolyte containing 0.1 M NH<sub>4</sub>F and 1 M H<sub>2</sub>O under self-organized conditions (Experimental details are provided in the ESI†). Fig. 1a–d shows scanning electron microscope (SEM) images (top view and cross section) of TiO<sub>2</sub> and 0.1 wt% Nb-doped TiO<sub>2</sub> nanotube layers formed on pure Ti and a Ti–0.1Nb alloy. This anodization process was found to lead over the entire investigated Nb-concentration range to the formation of smooth and uniform self-organized oxide layers. The tubes are open on the top and closed at the bottoms (inset of Fig. 1c). As in most cases of TiO<sub>2</sub> nanotube formation, a thin porous layer (initiation layer) is present<sup>16</sup> on the top of the tubes. This layer is some 10 nm thick with a very regular tube layer underneath. The tube length shown in Fig. 1 is approx. 2 μm but it easily can be controlled ranging from 1 μm to 15 μm by varying the anodization time from 5 min to 2.5 h. It is noteworthy that to achieve the same thickness of a nanotube layer on the 0.1Nb–Ti alloy it takes twice the anodization time of pure Ti. This indicates that the anodization properties of Nb (even at low Nb concentration) are strongly affecting the metal to oxide (tube) conversion, as shown in ESI†, Fig. S3.

All as-formed tubular oxide structures were amorphous but could be crystallized by an adequate heat treatment. Fig. 1e shows X-ray diffraction patterns (XRD) of as-formed tubes after annealing at 450 °C and 650 °C for 3 h in air. At 450 °C the heat-treatment converts the doped and the reference layers mainly to anatase TiO<sub>2</sub>. A small peak corresponding to the rutile phase at 2θ = 27.3° is found for the 0.1Nb-doped sample.

<sup>a</sup> Department of Materials Science, WW4-LKO, University of Erlangen-Nuremberg, Martensstrasse 7, D-91058 Erlangen, Germany. E-mail: schmuki@ww.uni-erlangen.de; Fax: +49 9131 852 7575; Tel: +49 9131 852 7582

<sup>b</sup> Helmholtz-Zentrum Geesthacht, Zentrum für Material-und Küstenforschung GmbH, Max-Planck-straße 1, 21502, Geesthacht, Germany. E-mail: jonathan.paul@gkss.de

† Electronic supplementary information (ESI) available: Experimental details, DSSC characteristics, XPS analysis, and SEM images of the samples. See DOI: 10.1039/c0cc04993j

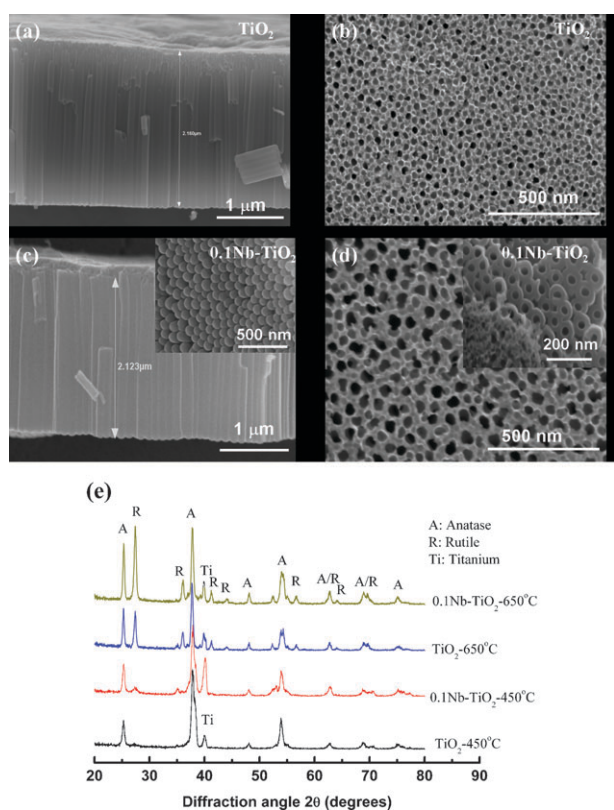


**Fig. 1** (a)–(d) SEM images of oxide nanotube layers grown on pure Ti (a, b) and a 0.1 wt% Nb–Ti alloy (c, d). (e) XRD patterns of 0.1Nb–TiO<sub>2</sub> and TiO<sub>2</sub> nanotubes after annealing in air at different temperatures.

Annealing at 650 °C leads to considerable rutile formation. It is apparent that stronger rutile peaks are observed in 0.1Nb-doped TiO<sub>2</sub> than in the pure TiO<sub>2</sub> sample. The reason for annealing at 650 °C is that previous work showed that amorphous Nb-oxides can be crystallized at 650 °C to a pseudo-hexagonal Nb<sub>2</sub>O<sub>5</sub>.<sup>17</sup> In the present case, due to the low doping concentration, this crystallization process of the Nb phase cannot be detected in XRD. The presence of Nb<sub>2</sub>O<sub>5</sub> in tubes, however, can be confirmed using X-ray photoelectron spectroscopy (XPS), as illustrated in Fig. S1 of ESI.† As apparent, the peak positions of Nb 3d are located at 207.13 and 209.73 eV, which are consistent with the formation of Nb<sub>2</sub>O<sub>5</sub>. The concentration is found to be 1.4 wt%, *i.e.* no significant concentration changes to the substrate occur during oxidation (*e.g.* due to selective dissolution).

In order to examine the effect of Nb doping on the DSSC performance, solar cells were assembled as described in ref. 8 using 2 μm long oxide tubes with different Nb contents using samples annealed at 450 °C and 650 °C. The DSSC performance was characterized by *I*–*V* curves using an AM 1.5 solar simulator setup—the results are summarized in Fig. 2 and Table S1 (ESI†). The amount of dye-loading was measured in all samples and was found not to vary significantly. Details on the experimental procedure and set-up are given in the ESI.† From the results of Fig. 2 it is clear that the Nb content and the crystallinity of oxide have a significant effect on the solar cell performance. Most remarkable is that the highest energy-conversion efficiency of 3.21% is achieved for a DSSC based on a 0.1Nb-doped TiO<sub>2</sub> nanotube layer annealed at 450 °C, *i.e.* the efficiency is 34% higher than for the undoped TiO<sub>2</sub> reference sample. The results

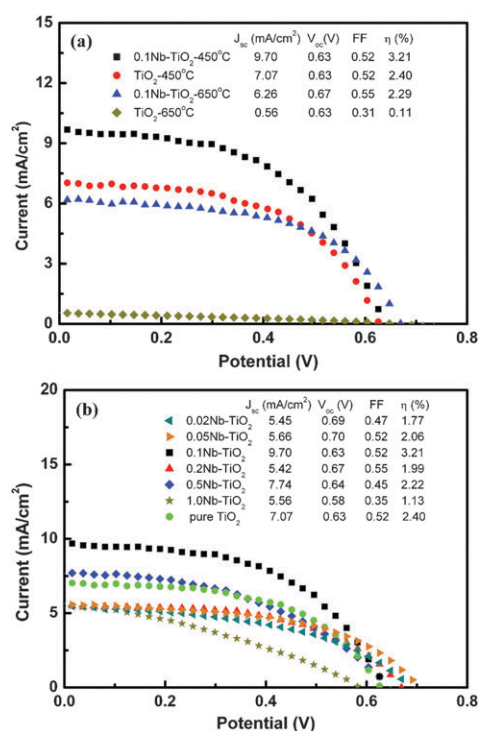


**Fig. 2** *I*–*V* characteristics for DSSCs fabricated using (a) TiO<sub>2</sub> and 0.1Nb–TiO<sub>2</sub> nanotubes annealed at different temperatures. (b) different concentrations of Nb doping in TiO<sub>2</sub> nanotubes annealed at 450 °C. The inset data give extracted solar cell parameters ( $J_{sc}$  = short-circuit current,  $V_{oc}$  = open-circuit voltage, FF = fill factor,  $\eta$  = efficiency).

also show that a Nb content of 0.1% represents a maximum beneficial effect, neither higher nor lower Nb contents were found to be effective. As expected, samples containing a higher amount of anatase show a higher efficiency in DSSCs (as well established for pure TiO<sub>2</sub>).<sup>8</sup> This is actually ascribed to an electron mobility that is approximately 10 times higher for anatase than for rutile.<sup>18</sup> For the Nb doped samples after annealing at 650 °C, a mixture of anatase and rutile phase is observed. However, in the case of pure TiO<sub>2</sub> nanotubes the efficiency strongly decreases to 0.11% after 650 °C heat-treatment. In contrast, the detrimental effect of the rutile is much less pronounced for the Nb doped sample, where the efficiency decreases only from 3.21% to 2.29% (see Fig. 1e).

In order to investigate the possible origins of the beneficial effect of Nb doping, the charge transport and recombination characteristics of the solar cells were measured using intensity modulated photovoltage spectroscopy (IMVS) and photocurrent spectroscopy (IMPS). The efficiency of a solar cell in terms of the collection efficiency  $\eta$  can be considered to be given by  $\eta = 1 - \tau_c/\tau_r$ .<sup>19</sup> From the spectroscopic data the recombination ( $\tau_r$ ) and the transport time ( $\tau_c$ ) constants were evaluated as described in the ESI.† Fig. 3a and b shows  $\tau_r$  and  $\tau_c$  as a function of the incident photon flux (light intensity)<sup>20</sup> for DSSCs based on nanotube layers annealed at 450 °C for the 0.1Nb doped (with the highest DSSC efficiency) and the non-doped reference sample. Clearly, both recombination time and transport time become shorter with an increasing light intensity, which corresponds to a decrease of the electron lifetime and transit time, respectively. The most significant difference between pure TiO<sub>2</sub> and the Nb doped material is

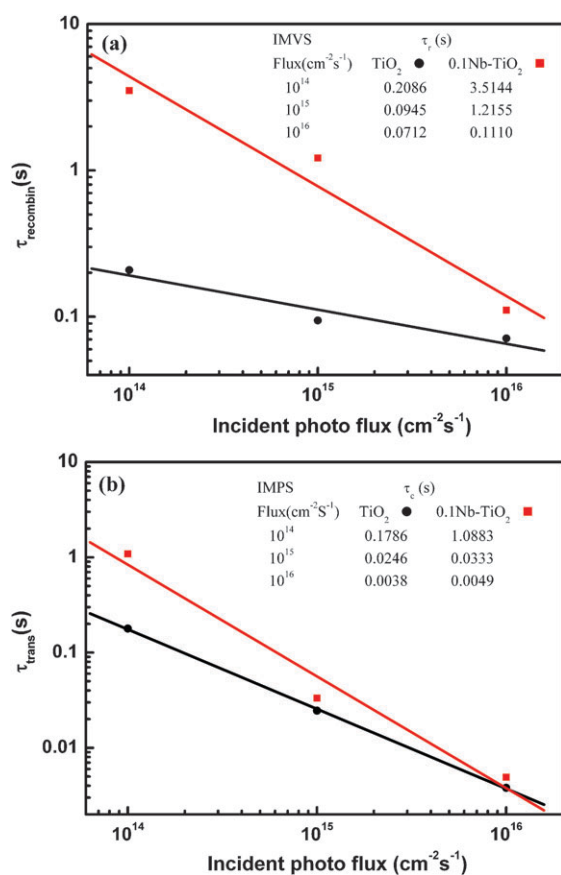


**Fig. 3** (a) Recombination time ( $\tau_r$ ) and (b) electron transfer ( $\tau_c$ ) constants calculated from IMVS and IMPS measurements for pure TiO<sub>2</sub> and 0.1Nb-TiO<sub>2</sub> nanotube layers shown in Fig. 1 after annealing at 450 °C.

apparent from IMVS. A much higher recombination time constant is observed in Nb-doped TiO<sub>2</sub> nanotubes, as shown in Fig. 3a, *i.e.* in the Nb doped tubes the electron life-time is much higher than that in pure TiO<sub>2</sub>—at low levels of light illumination the difference is particularly striking (for example,  $\tau_r$  is 17 times higher for the Nb doped material at a photon flux of 10<sup>14</sup> cm<sup>-2</sup> s<sup>-1</sup>). For the overall efficiency this means that although a slightly faster electron transfer takes place in the pure TiO<sub>2</sub> nanotube layer (as apparent from the slightly lower  $\tau_c$  in Fig. 3b), the significantly higher recombination rate constant for the Nb doped sample leads to an overall higher electron collection efficiency, *i.e.*, the beneficial effect of Nb doping must be ascribed to the suppression of recombination effects. It is reported that higher conductivity for low Nb-doped TiO<sub>2</sub> can be attributed to small static effective mass, high ionization efficiency of Nb, and large dielectric constant.<sup>21</sup> All these electronic effects may contribute to deactivate charge recombination pathways of electrons from the TiO<sub>2</sub> *via* surface or bulk state recombination.

Considering the overall efficiency of ~3% it should be noted that the present results were obtained with a solar cell arrangement that was selected to demonstrate the effect of Nb doping in TiO<sub>2</sub> nanotube layers—the construction is far from being optimized considering other crucial factors affecting the solar cell efficiency (such as surface morphology of the tubes,<sup>9,22,23</sup> or additional particle loading,<sup>8</sup> or length and

diameter of the tubes<sup>8</sup>). Nevertheless, the present findings demonstrate that using low level Nb-doping of TiO<sub>2</sub>, a significant enhancement in TiO<sub>2</sub> nanotube based DSSCs can be achieved.

In summary, self-ordered Nb-doped TiO<sub>2</sub> nanotube layers were successfully fabricated by anodization of Ti-Nb alloys under optimized electrochemical conditions. Compared with self-organized arrays of pure TiO<sub>2</sub> nanotubes, Nb-doped nanotubes can exhibit a remarkable enhancement in efficiency when used in DSSCs. Based on IMVS and IMPS data the beneficial effect is ascribed to considerably improved recombination characteristics observed for the Nb doped nanotubes.

For financial support the authors are thankful to the Alexander von Humboldt Foundation (for H. Jha), German Science Foundation (DFG) and DFG Cluster of Excellence (EAM). Prof. Dr Florian Pyczak and Dr Michael Oehring at Helmholtz-Zentrum Geesthacht (Geesthacht, Germany) are acknowledged for providing the Ti-Nb alloys. Helga Hildebrand and Ulrike Marten-Jahns are also acknowledged for XPS and XRD measurements.

## Notes and references

- B. O'Regan and M. Grätzel, *Nature*, 1991, **353**, 737–740.
- J. Nelson, *Phys. Rev. B: Condens. Matter Mater. Phys.*, 1999, **59**, 15374–15380.
- L. M. Peter, *J. Phys. Chem. C*, 2007, **111**, 6601–6612.
- M. Adachi, Y. Murata, J. Takao, J. Jiu, M. Sakamoto and F. Wang, *J. Am. Chem. Soc.*, 2004, **126**, 14943–14949.
- J. B. Baxter and E. S. Azdil, *Appl. Phys. Lett.*, 2005, **86**(5), 1–3, art. no.053114.
- K. Fujihara, A. Kumar, R. Jose, S. Ramakrishna and S. Uchida, *Nanotechnology*, 2007, **18**, 365709.
- S. H. Kang, S. H. Choi, M. S. Kang, J. Y. Kim, H. S. Kim, T. Hyeon and Y. E. Sung, *Adv. Mater.*, 2008, **20**, 54–58.
- P. Roy, D. Kim, K. Lee, E. Spiecker and P. Schmuki, *Nanoscale*, 2010, **2**, 45–59.
- K. Zhu, N. R. Neale, A. Miedaner and A. J. Frank, *Nano Lett.*, 2007, **7**(1), 69–74.
- J. R. Jennings, A. Ghicov, L. M. Peter, P. Schmuki and A. B. Walker, *J. Am. Chem. Soc.*, 2008, **130**, 13364–13372.
- A. Ghicov and P. Schmuki, *Chem. Commun.*, 2009, 2791–2808.
- D. Morris, Y. Dou, J. Rebane, C. E. J. Mitchell, R. G. Egdell, D. S. L. Law, A. Vittadini and M. Casarin, *Phys. Rev. B: Condens. Matter Mater. Phys.*, 2000, **61**(20), 13445–13457.
- M. Lira-Cantu, M. K. Siddiki, D. Muñoz-Rojas and R. Amade, *Sol. Energy Mater. Sol. Cells*, 2010, **94**, 1227–1234.
- Y. Furubayashi, T. Hitosugi, Y. Yamamoto, K. Inaba, G. Kinoda, Y. Hirose, T. Shimada and T. Hasegawa, *Appl. Phys. Lett.*, 2005, **86**, 252101.
- T. Hitosugi, A. Ueda, Y. Furubayashi, Y. Hirose, S. Konuma, T. Shimada and T. Hasegawa, *Jpn. J. Appl. Phys.*, 2007, **46**, L86–L88.
- H. Tsuchiya, J. M. Macak, A. Ghicov and P. Schmuki, *Small*, 2006, **2**, 888–891.
- A. Ghicov, S. Aldabergenova, H. Tsuchiya and P. Schmuki, *Angew. Chem., Int. Ed.*, 2006, **45**, 6993–6996.
- H. Tang, K. Prasad, R. Sanjinbs, P. E. Schmid and F. Levy, *J. Appl. Phys.*, 1994, **75**, 2042–2047.
- G. Schlichthorl, N. G. Park and A. J. Frank, *J. Phys. Chem. B*, 1999, **103**, 782–791.
- G. Schlichthorl, S. Y. Huang, J. Sprague and A. J. Frank, *J. Phys. Chem. B*, 1997, **101**, 8141–8155.
- Y. Furubayashi, N. Yamada, Y. Hirose, Y. Yamamoto, M. Otani, T. Hitosugi, T. Shimada and T. Hasegawa, *J. Appl. Phys.*, 2007, **101**, 093705.
- D. Kim, A. Ghicov, S. P. Albu and P. Schmuki, *J. Am. Chem. Soc.*, 2008, **130**(49), 16454–16455.
- P. Roy, D. Kim, I. Paramasivam and P. Schmuki, *Electrochem. Commun.*, 2009, **11**, 1001–1004.